ARTICLE

Hydrophobicity Optimization of Cathode Catalyst Layer for Proton Exchange Membrane Fuel Cell

Hao-Jie Chen, Mei-Hua Tang, Sheng-Li Chen*

Hubei Key Laboratory of Electrochemical Power Sources, Department of Chemistry, Wuhan University, Wuhan 430072, China

Abstract

Hydrophobicity of the cathode catalyst layers (CCLs) crucially determines the performance of proton exchange membrane fuel cells (PEMFCs) by affecting the transports of oxygen and liquid water. In this regard, polytetrafluoroethylene (PTFE) is usually used as a hydrophobic additive to facilitate the oxygen and water transports in CCLs. So far, there remains lacking systematic effort to optimize the addition methods of PTFE in CCLs and the mechanisms behind. In this work, the effects of the approaches for PTFE addition and the distribution of PTFE on the mass transport of oxygen and the proton conduction in CCLs were studied by using a number of electrochemical characterization methods and contact angle tests. It was found that direct adding PTFE molecules is a better way than adding the PTFE-modified carbons to improve the electrochemical properties of CCLs, since the latter causes an increase in the proton transport resistance, whereas the direct molecule addition results in the obviously improved oxygen transport without affecting the proton conduction. In addition, the gradient distribution of PTFE in CCLs, more specifically, adding PTFE near the interface between CCL and gas diffusion layer (GDL), yielded higher catalyst utilization than the homogeneous distribution of PTFE due to the lower oxygen transport resistance.

Keywords: Proton exchange membrane fuel cells; Cathode catalyst layer; Hydrophobicity; Polytetrafluoroethylene; Oxygen transport resistance

1. Introduction

The development of environmentally friendly energy technology has been the common pursuit of the society to cope with the global warming problems causing by fossil fuel consumption. Among the various energy systems, proton exchange membrane fuel cells (PEMFCs) have received widespread attention for their high energy density, high energy conversion efficiency, low operating temperature, and almost zero emission [1,2]. However, the cost of PEMFCs is a serious constraint to their commercialization, and in order to reduce costs, it is especially critical to improve catalyst utilization [3]. As the core component of PEMFC, the membrane electrode assembly (MEA) is the site where the electrochemical reaction takes place directly, and its structure directly affects the catalyst utilization [4]. Compared with the anode catalyst layer where the fast hydrogen oxidation reaction (HOR) occurs, the design of cathode catalyst layer (CCL) structure requires more consideration for its sluggish kinetics of oxygen reduction reaction (ORR) and complex gas-liquid transport process [5]. At high current densities, the formation of liquid water inside could substantially hinder the oxygen transport and cause a significant voltage drop during operation [6]. Therefore, to facilitate the flowing of water and increase the accessibility of oxygen to platinum (Pt), it is necessary to optimize the hydrophobic structure of the CCLs.

Most of research to optimize the hydrophobicity is to add PTFE to the CCL [3,7,8]. Chi et al. [8] prepared MEAs containing different PTFE loadings and found that the appropriate amount of PTFE could significantly enhance the performance and stability of MEA. They concluded that the increased hydrophobicity of CCL effectively

Received 6 July 2022; Received in revised form 14 July 2022; Accepted 20 July 2022
Available online 21 July 2022

* Corresponding author, Sheng-Li Chen, Tel: (86-27)68754693, E-mail address: slchen@whu.edu.cn.

https://doi.org/10.13208/j.electrochem.2207061

removed the excess water and the reaction gas could reach the reaction site more easily. Avcioglu et al. [7] used a two-step method to add PTFE into the CL to construct hydrophobic mesoporous channels, which reduced the oxygen transport resistance at large current densities and increased the power density of the MEA. However, the MEA performance decreased dramatically when the PTFE loading exceeded a certain amount, which is generally attributed to the excess PTFE covering the active sites of the catalyst and reducing the Pt utilization [9]. To avoid the disorderly distribution of PTFE within the CL, some composite hydrophobic additives formed by pretreatment of PTFE have also been applied to the CL to improve the water management. Wang et al. [10] combined PTFE and solid carbon particles (XC72) at high temperature to make a special strongly hydrophobic carbon material, achieving the goal of constructing hydrophobic gas transport channels without affecting the catalyst activity. Similarly, Cai et al. [11] combined PTFE and carbon nanotubes (CNTs) to generate CNTs@PTFE, which were added to the CL to improve water management.

These studies, as mentioned above, focused on tuning the hydrophobicity/hydrophilicity balance. Another strategy for improving PEMFCs performance and water management is to design the CCLs structure [12−14]. Lee et al. [12] prepared a double CCL structure of MEA with a hydrophilic outer layer and a hydrophobic inner layer, which was used for PEMFC at low relative humidity. They found that the MEA with a double-layer CCL had higher performance and lifetime than MEA with a single hydrophobic CL or a single hydrophilic CL. A double CCL structure MEA with a hydrophilic inner layer and a hydrophobic outer layer was designed by Qiu et al. [13]. Compared with the conventional single-CCL structure, this double-layer structure produced better Pt utilization, reduced interfacial resistance between CL and GDL, and enhanced gas transport, resulting in a better performing MEA. However, most studies usually focus only on the improvement on the polarization curve and the mechanisms behind have persisted incomplete.

In this work, we firstly optimized the PTFE addition method by catalyst coated membrane (CCM) method, and then investigated the effects of direct PTFE addition and hydrophobic carbon after PTFE treatment on the MEA performance by electrochemical characterizations, and discussed the influencing mechanisms of both proton transport and oxygen transport. Further, based on the optimization results, a special CL structure with the gradient distribution of PTFE was designed to investigate the effect of different PTFE distribution positions on the MEA performance.

2. Experimental

2.1. Preparation of MEAs

The active area of all the MEAs used in this study was 4 cm^2. Firstly, 40 wt% Pt/C catalyst (Johnson Matthey) and 5 wt% Nafion solution (DuPont D520, USA) were dispersed into isopropyl alcohol, and then the mixture was sonicated for 120 min to ensure uniform dispersion. Afterwards, the required amount of hydrophobic additive (PTFE or PTFE@XC72) was added to the CCL ink and sonicated for 30 min. The catalyst ink was then sprayed on both sides of the proton exchange membrane (NR211, DuPont, USA) using a gas-assisted spraying method and heated at 80 °C to evaporate the solvent to produce CCM. The loadings of Pt on the anode and cathode were 0.1 and 0.2 $mg \cdot cm^{-2}$, respectively, and the mass ratio of ionomer/carbon was 0.5 (Figure S1 shows that the optimal mass ratio of ionomer/carbon was 0.5). Finally, MEAs were prepared by assembling the CCM and the anode/cathode GDL (Ballard).

PTFE is a stable and high temperature resistant polymer with a wide range of applications in the MEA. Therefore, we believe that the addition of PTFE into the CL will not adversely affect the stability of the PEMFC.

The parameters of the different MEA samples prepared in this work are presented in Table 1. It is worth noting that "In" and "Out" in the sample names refer to the distributions of the additives close to the PEM and close to the GDL, respectively. For example, in the case of "MEA+0.1 P-Out", a total of 0.1 PTFE/carbon mass ratio of 0.5 wt% PTFE emulsion (Aladdin) was added in the CL, and all PTFE was distributed in the CL near the GDL.

2.2. Preparation of PTFE@XC72

A certain amount of XC72 was weighed in a beaker, and a mixture of ethanol and ultrapure water was taken to submerge XC72 with the volume ratio of 3:7 of ethanol to water. After an ultrasonic dispersion, 0.5 wt% PTFE emulsion was added drop by drop, the amount of PTFE emulsion required was

Table 1. Detailed information of fabricated CCMs.

Sample	Type of additive	Loading of additive
control MEA	–	–
MEA+0.1 P	PTFE	PTFE/Carbon = 10 wt%
MEA+0.36mgPC	PTFE@XC72	0.36 mgPC
MEA+0.1 P-Out	PTFE	PTFE/Carbon = 10 wt%

twenty percent of the mass of XC72 to calculate the volume of PTFE. After the dropwise addition, the sonication was continued until it was as disperse as possible, and ethanol was added dropwise under sonication oscillation until the volume ratio of ethanol to water became 4:1. The mixed solution was evaporated at 130 °C and PTFE was attached to the carbon surface. The resulting product was calcined at 330 °C for half an hour in an argon atmosphere to obtain PTFE@XC72 solid particles, named PC.

The prepared PC and solid carbon XC72 powders were adhered to the conductive adhesive, and their microscopic morphology was characterized by SEM. As shown in Figure S2, the particle sizes of hydrophobic carbon and XC72 nanoparticles were similar, and there was no significant change in the morphology and no large PTFE agglomerates appeared, indicating that this hydrophobic carbon preparation method could achieve uniform distribution of PTFE on carbon.

2.3. Physical characterizations

The surface hydrophobicity of the CCL was characterized by an optical contact angle meter. 5 μL water droplet was dropped on the surface of the sample with a microinjector at room temperature, the surface contact angle was obtained by photographing.

Scanning electron microscope (SEM, zeiss Merlin Compact) was principally applied to examine the surface morphology of MEAs. As shown in Figures S3 and S4, all CLs had similar surface structures, i.e., a porous structure composed of catalyst and ionomer. Among them, all the catalysts in the CLs prepared by different hydrophobicity optimization methods were very uniformly dispersed with no appearance of large agglomerates.

2.4. MEA electrochemical characterization

The electrochemical performance of the MEA was evaluated through polarization curve (*i-V* curve) measurements on the Scribner 850e fuel cell system equipped with a load and frequency analyzer. The cell temperature was set to be 80 °C with pure H_2 and O_2 externally humidified (100% RH) being fed to the anode and cathode, respectively. Gas flow rates were constant at 0.6 $L \cdot min^{-1}$ for both the electrodes. The electrochemical impedance spectra (EIS) were tested at 10 kHz−0.1 Hz with a sine wave potential amplitude of 10 mV.

The proton transport resistance in the CL was measured at 80 °C using EIS [15]. H_2 (100%RH) and N_2 (100%RH) were supplied at the anode and cathode, respectively, at flow rates of 0.2 $L \cdot min^{-1}$. Nyquist plots were recorded by BioLogic SP300 in the potentioststic EIS mode at 0.4 V with the AC amplitude of 15 mV from 100 kHz to 1 Hz.

The electrochemical surface area (ECSA) was measured by cyclic voltammetry (CV) using a potentiostat (CorrTest). The gas flow rates of H_2/N_2 for both the anode and cathode were 0.2 $L \cdot min^{-1}$ at 80 °C and 100%RH. The hydrogen-fed anode was used as both the reference electrode and counter electrode. The cathode as the working electrode was swept from 0.1 to 1.23 V and then back to 0.1 V at a potential scan rate of 500 $mV \cdot s^{-1}$. The cycle was repeated until no change in the CV shape was observed, and then 5 cycle scans were obtained. The ECSA was calculated from integral charges corresponding to the hydrogen atom adsorption ranging from 0.1 to 0.4 V.

The limiting current method was used to test the oxygen transport resistance by stepping from the open circuit potential to 0.1 V at a rate of change of 5 $mV \cdot s^{-1}$ and then returning to the open circuit potential at the same rate, and repeating five times to obtain the limiting current. The limit currents were tested at the three pressures of 100 kPa, 150 kPa and 200 kPa, and four oxygen concentrations of 1%, 2%, 4% and 8%. The slope of the straight line obtained by fitting the limiting current to the oxygen concentration gives the oxygen transfer resistance of the CL.

3. Results and discussion

3.1. Effects of PTFE addition methods

First, we investigated the effect of PTFE addition on the electrochemical performance of the MEA. From Fig. 1(a), it can be seen that with the increase of PTFE content in the CCL, the peak power density first increases and then decreases, indicating that the proper amount of PTFE enhances the MEA performance, while the excessive amount of PTFE weakens the MEA performance. The best MEA performance was obtained when the mass ratio of PTFE/carbon (P/C) was 0.1, showing the current densities of 320, 2300, and 4261 $mA \cdot cm^{-2}$ at 0.8, 0.6, and 0.4 V, respectively; and 337 mA cm^{-2} higher at 0.4 V than the MEA without PTFE in the CCL. From the polarization curves, the addition of PTFE mainly raised the performance in the large current range, which seems to be similar to the reported results [9]. As shown in Fig. 1(b), the CV curves also show the same trend as the performance, that is, the ECSA increasing from 236 $cm^2 \cdot mg^{-1}$ to 255 $cm^2 \cdot mg^{-1}$ with P/C = 0.1, and then decreasing to 201 $cm^2 \cdot mg^{-1}$ with P/C = 0.2. At P/C = 0.2, both the MEA performance and ECSA were reduced, because the excess PTFE might cover some Pt active sites, increasing the charge transfer resistance, and at the same time, it might block some of

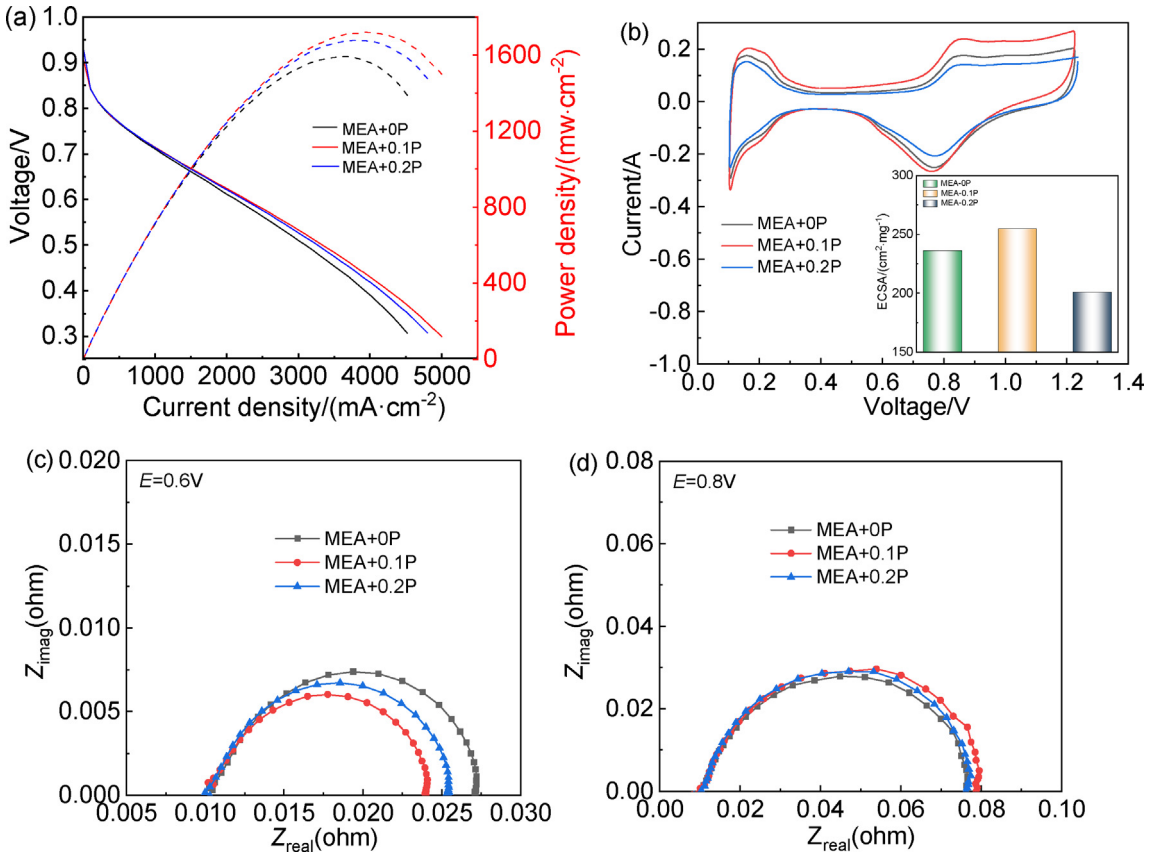

Fig. 1. Electrochemical responses of MEAs with different PTFE contents: (a) polarization and power density curves; (b) CVs and ECSA plots; (c) EIS at E = 0.6 V; (d) EIS at E = 0.8 V.

the pore, making the reaction gas transport limited [8].

Fig. 1(c and d) shows the EIS of MEAs with different PTFE contents. The high frequency intersection of the semicircle on the horizontal axis is the high frequency resistance (HFR), which indicates the total ohmic resistance of the MEA (R_Ω) [16]. Generally, the ohmic resistance of MEA is mainly related to the proton conductivity of PEM and the conductivity of the CL. It can be seen that the HFR data of each MEA are almost the same at 0.8 V and 0.6 V. This indicates that the small amount of PTFE has little effect on the conductivity of the CL. At 0.8 V, as shown in Fig. 1(d), different MEAs present similar impedance semicircle sizes. At this time, the current density is low and electrochemical polarization occupies the major part of the polarization loss, which indicates that the proper amount of PTFE has no significant effect on the activity of the catalyst. As the cell voltage decreased from 0.8 V to 0.6 V, the current density increases and the diameter of the semicircle in the Nyquist plot decreases. Fig. 1(c) shows the decreased EIS semicircle diameter in an order: MEA+0 P > MEA+0.2 P > MEA+0.1 P. This corresponds to the polarization curve, where the MEA with lower resistance has a better performance. This indicates that the addition of PTFE improves mainly the resistance at large current density which may be due to the improvement of gas-liquid transport channels.

As can be seen in Fig. 1, the addition of PTFE mainly improves the performance at large current density when mass transfer is the main factor affecting the performance of MEA. In order to investigate the reason for the improvement of PTFE on the MEA performance, the proton transfer resistance and oxygen resistance were characterized, as shown in Fig. 2. It obviously demonstrates that the oxygen transport resistance of the MEA containing PTFE is significantly lower than that of the control MEA. By inverting the linear relationship between oxygen transport resistance and gas pressure to zero pressure, the pressure-independent resistance (R_{np}) is obtained, which is mainly related to the oxygen transport in CCL. As shown in Fig. 2(b), the R_{np} followed by the order of MEA+0 P (0.78 s·cm^{-1}) > MEA+0.2 P (0.72 s·cm^{-1}) > MEA+0.1 P (0.56 s·cm^{-1}), indicating that PTFE improves the oxygen transport in the CL. The addition of PTFE is beneficial to both the diffusion of the oxygen in the CL and the gas-liquid transport channels within the CL. Fig. 2(c and d) shows the results of the proton

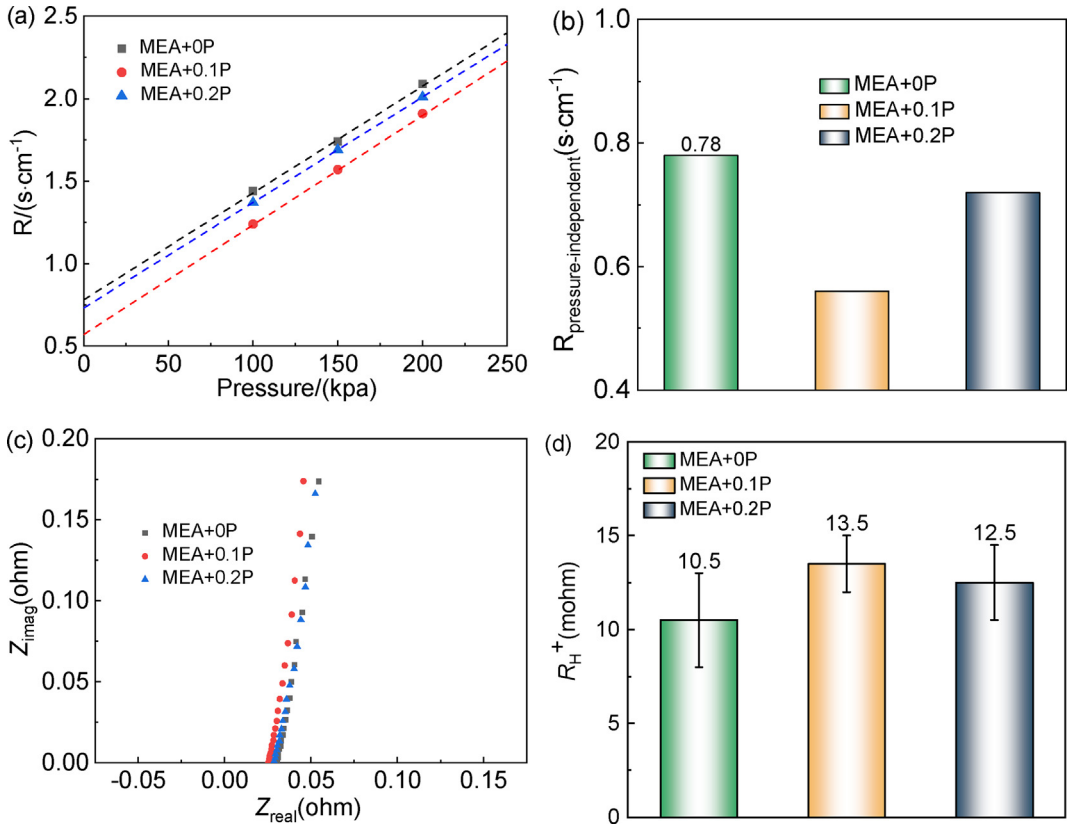

Fig. 2. The graphs showing oxygen transport resistances (a—b) and proton transport resistances (c—d) of MEAs with different PTFE contents.

transport resistance test. As can be seen from the figures, the addition of PTFE has no significant effect on the proton transport resistance. This indicates that the improvement of performance in the MEA is mainly due to the reduction in oxygen transport resistance.

To avoid the disordered distribution of PTFE in the CL, PC (PTFE@XC72) was added to the CL. As shown in Fig. 3(a), the MEA+0.36mgPC exhibited the highest current density of 4185 $mA \cdot cm^{-2}$ at 0.4 V, which was 261 $mA \cdot cm^{-2}$ higher than that of the control MEA. The polarization curve with the PC addition is the same as the MEA with the PTFE addition, and the addition of PC also mainly improves the performance at large current density. The CV test results (Fig. 3(b)) show that the addition of PC increased the ECSA value of the MEA to 266 $cm^2 \cdot mg^{-1}$, which improved the catalyst utilization. The performance improvement of the MEA with the PC addition was less than the expected as compared to that of the MEA with the direct PTFE addition, which may be due to the carbon particles increasing the thickness of the CL, resulting in a longer transport path of the reactant material. As shown in Fig. 3(c and d), the HFR values were almost constant at 0.6 V and 0.8 V, which indicates that the addition of PC has little effect on the conductivity of the CL.

As shown in Fig. 4(a—b), the R_{np} values of the MEA with three different PC contents were 0.78, 0.74 and 0.80 $s \cdot cm^{-1}$, indicating that the oxygen transport resistance of the CL had a trend of decreasing and then increasing with the addition of PC. Fig. 4(c—d) shows that the proton transport resistance gradually increased from 10.5 mΩ to 21 mΩ with the increase of PC content in the CL relative to the control MEA. As seen in Figure S5, the increase in proton transport resistance might be caused by carbons, and PTFE could suppress this increase, i.e., reduce the proton transport resistance. This means that although the addition of PC can improve the channel of gas-liquid transport. However, when too much PC is added to the CL, the increase in the thickness of the CL will elongate the reaction material transport path, and thus increase the oxygen transport resistance and proton transport resistance. This is the reason why the effect of PC addition in MEA is not as effective as that of PTFE addition.

To further investigate the effect of the change of hydrophobicity of the CL surface on the MEA performance, the contact angle of liquid water on the surface of different CLs was characterized (as shown in Fig. 5), and the contact angle of the control CCL was 134.9°. As expected, the contact angle was increased after the addition of

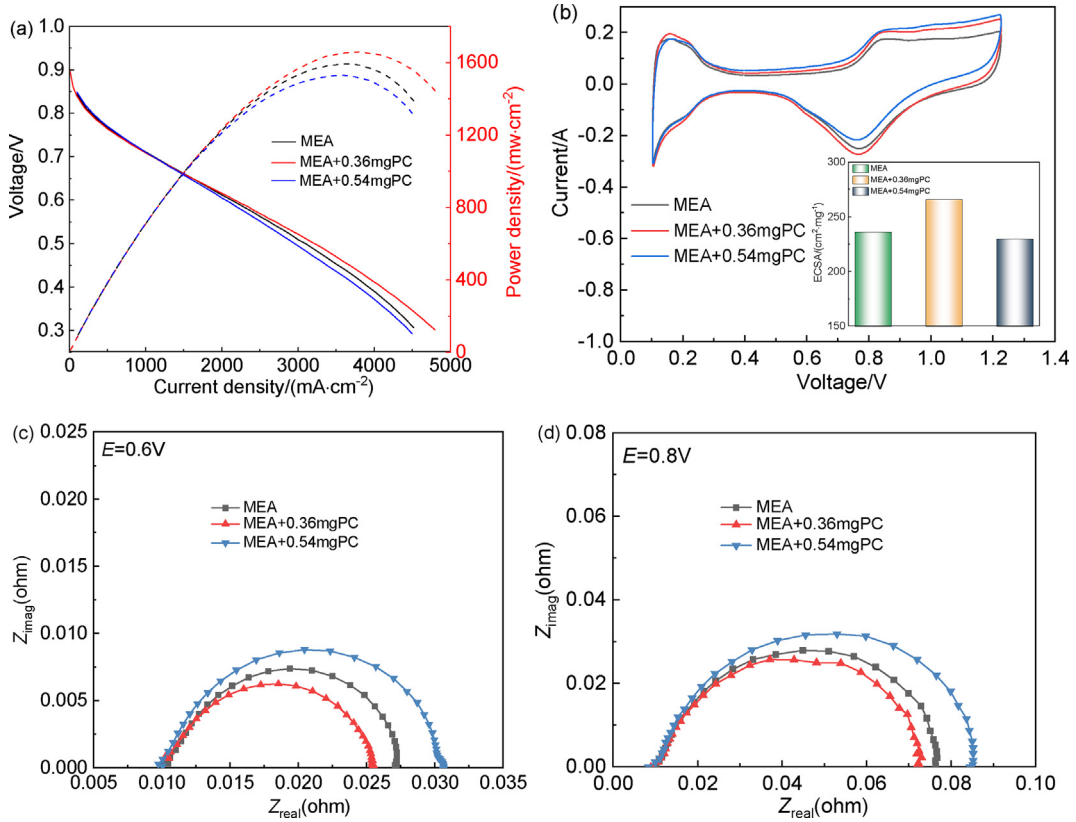

Fig. 3. Electrochemical responses of MEAs with different PC contents: (a) polarization and power density curves; (b) CVs and ECSA plots; (c) EIS at E = 0.6 V; (d) EIS at E = 0.8 V.

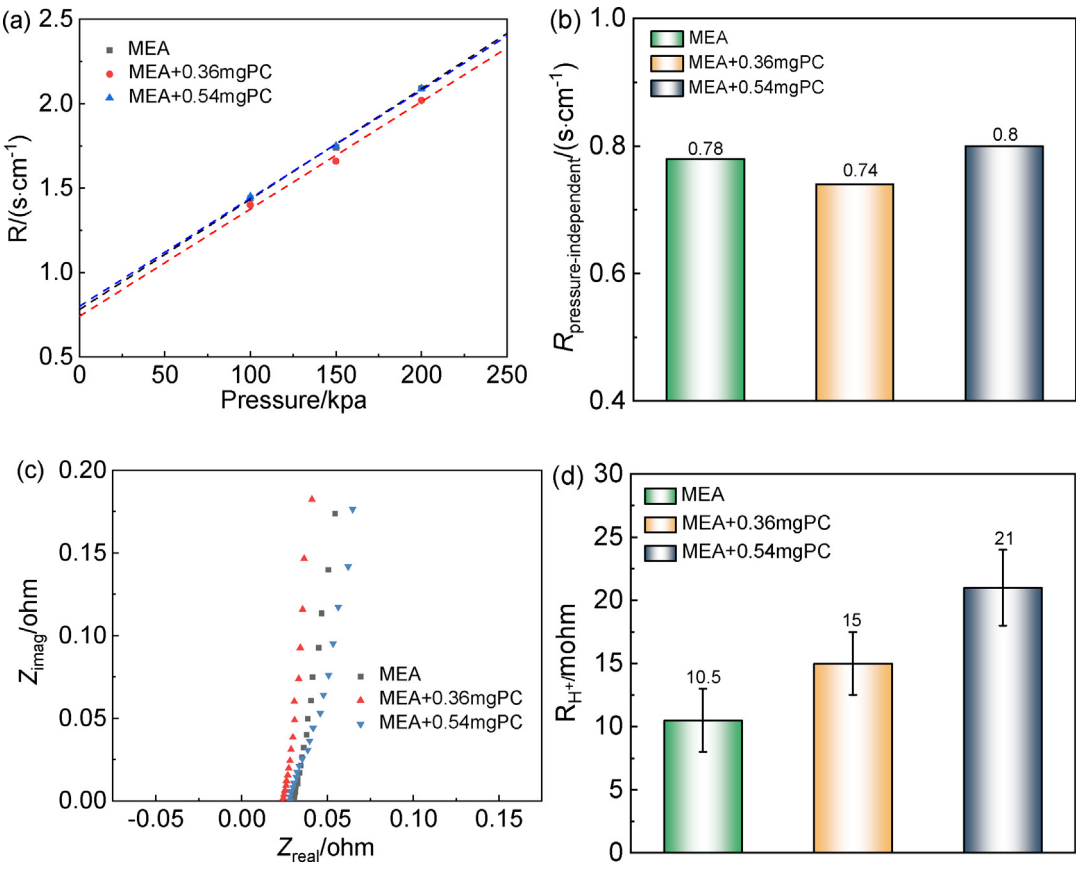

Fig. 4. The plots showing oxygen transport resistances (a—b) and proton transport resistances (c—d) of MEAs with different PC contents.

hydrophobic additives. In particular, the contact angle of the CL after the addition of PTFE was 138.5°, while that after the addition of PC was 145.8°. This indicates that both hydrophobic additives improved the gas-liquid transport channels within the CLs, where the hydrophobicity of PTFE and XC72 was improved even more after the heat treatment. The trends of polarization curve performance and contact angle were different, and the current density values of MEA+0.2 P and MEA+0.36mgPC were relatively close at each potential. This can indicate that the change of hydrophobicity on the CL surface is not the key to determine the MEA performance, while the changes of oxygen transport resistance and proton transport resistance within the CL are crucial.

3.2. Gradient distribution of PTFE

Based on the optimization of PTFE addition method, the effect of the gradient distribution of PTFE on the MEA was investigated by changing the distribution of PTFE in the CL. Fig. 6 shows the polarization curves, CV curves and EIS of the MEA with the gradient distribution of PTFE. As shown in Fig. 6(a), at P/C = 0.1, there is a decreasing tendency in the peak power density: MEA+0.1 P-Out > MEA+0.1 P-In > MEA+0.1 P. At 0.4 V, the current density of the MEA+0.1 P-Out was 426 $mA \cdot cm^{-2}$ and 515 $mA \cdot cm^{-2}$ higher than those of the MEA+0.1 P-In and MEA+0.1 P. This indicates that the gradient distributed structure near the GDL is more favorable for the performance improvement. With further increase in the PTFE content, this gap decreased to 154 $mA \cdot cm^{-2}$ and 396 $mA \cdot cm^{-2}$ in the MEA with P/C of 0.2 (Figure S6). In the previous results, the optimal ratio of PTFE was also 0.1. This means that when an excess PTFE is added to the CL, both the outer and inner distributions have a significant effect on the MEA performance. Local excess PTFE can block the gas-liquid transport channels and even cause agglomeration of the catalyst, thus hindering the reaction. The CV curves show that the CL structure with PTFE distributed close to the GDL has a higher catalyst utilization (Fig. 6(b)). This may be due to the fact that the gradient distributed structure creates a hydrophobic gradient, which facilitates the removal of liquid water and improves the gas transport. Fig. 6(c–d) shows the EIS data at 0.8 V and 0.6 V. As can be seen from the figure, the MEA+0.1 P-Out exhibited the lowest resistances at 0.6 V and 0.8 V, which is consistent with the polarization curves. In addition, all the EIS plots display the same high-frequency impedance responses, indicating that the gradient distribution of PTFE has a little effect on the electronic conductivity of the CL.

To further investigate the mechanism of the effect of the gradient PTFE distribution structure on the performance of the MEAs, the proton transport resistance and oxygen transport resistance tests were performed. From Fig. 7(a and b), it can be seen that the proton transport resistances of all the MEAs were close to each other, indicating that the effect of this structure on proton transport is not the main factor to improve the performance. Fig. 7(c and d) shows the test results of oxygen transport resistance, and it can be seen that the R_{np} of MEA+0.1 P-Out was 0.52 $s \cdot cm^{-1}$, while that of MEA+0.1 P-In was 0.78 $s \cdot cm^{-1}$. This difference of oxygen transport resistance is sufficient to illustrate the great influence of PTFE distribution location on oxygen transport. As mentioned earlier, the addition of PTFE in the CL near the GDL improves the construction of gas-liquid transport channels and accelerates the removal of liquid water inside the CL.

As shown in Fig. 8, the contact angle of MEA+0.2 P-Out was about 9° higher than that of MEA+0.2 P-In, while those of the CL within MEA+0.2 P-In and the control MEA were close to each other. This indicates that the PTFE distribution is as expected from the experiment, with almost all of the PTFE in MEA+0.2 P-Out being distributed in the CL near the GDL side, while nearly all of the PTFE in MEA+0.2 P-In being distributed in the CL near the PEM side, and no effect on the hydrophobicity of the CL near the outer side. In other words, the improved MEA performance is mainly caused by the gradient distribution of PTFE in the CL.

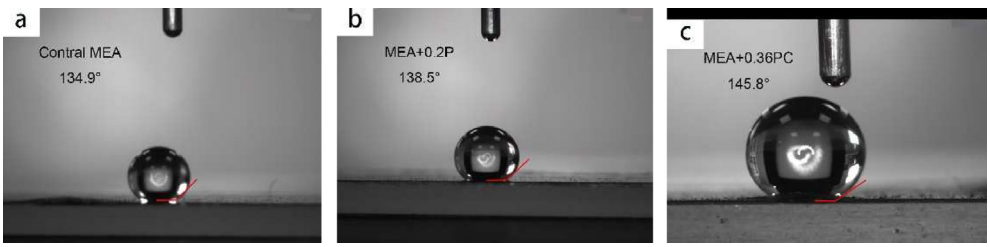

Fig. 5. Contact angles for CCLs containing various additives.

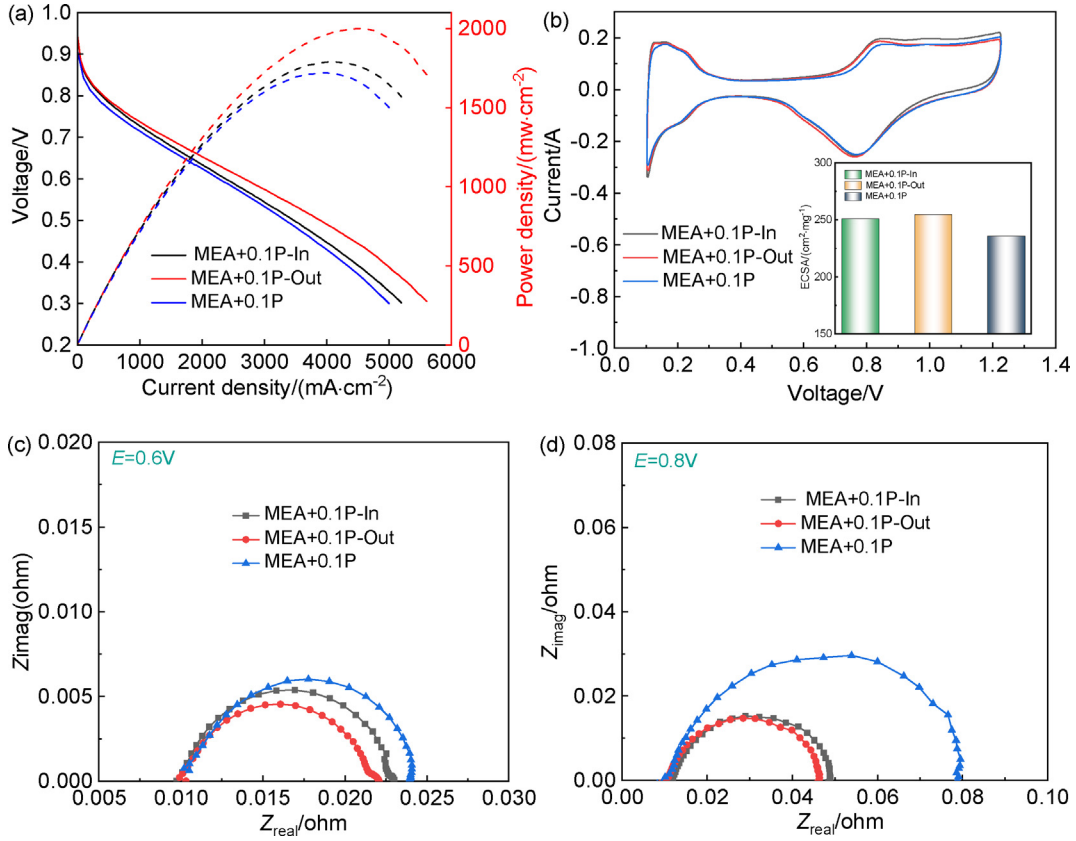

Fig. 6. Electrochemical responses of MEAs with the gradient distribution of PTFE: (a) polarization and power density curves; (b) CVs and ECSA plots; (c) EIS at E = 0.6 V; (d) EIS at E = 0.8 V.

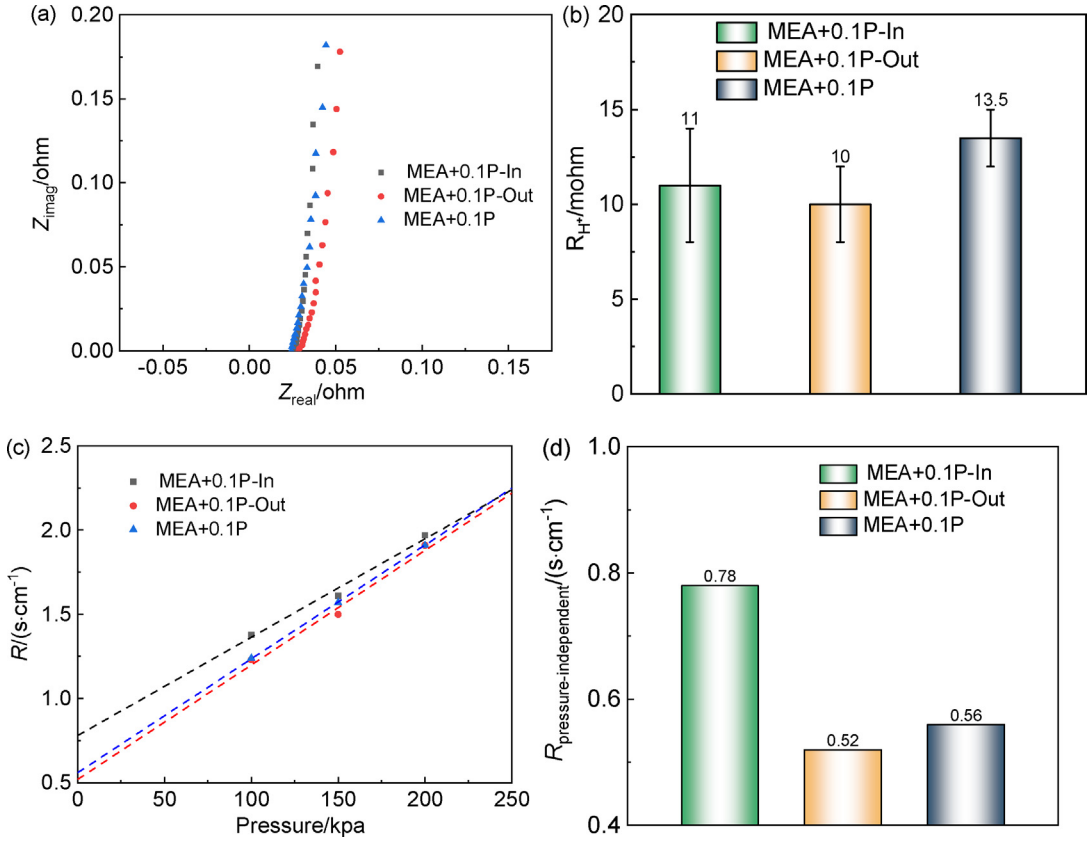

Fig. 7. The graphs showing proton transport resistances (a—b) and oxygen transport resistances (c—d) of MEAs with the gradient distribution of PTFE.

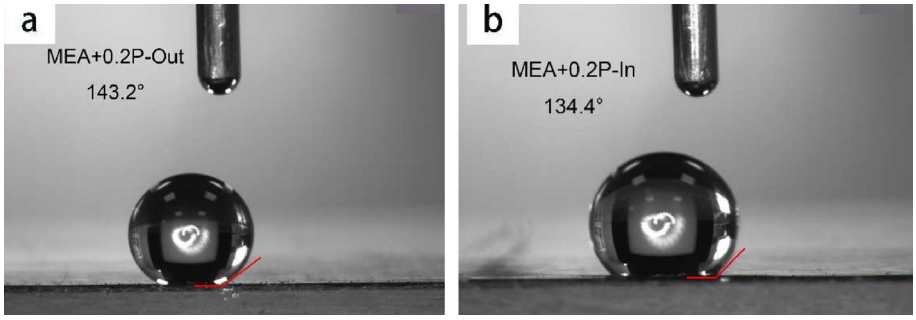

Fig. 8. Contact angles for CCLs containing the gradient distribution of PTFE.

4. Conclusions

In summary, we prepared a series of MEAs with different contents of additives, and conducted a detailed electrochemical and physical characterization. The results revealed that the optimal addition of PTFE had a predominant effect on the performance enhancement of the MEA, significantly reducing the oxygen transport resistance while maintaining the smooth proton transport in the CCL. In contrast, the addition of hydrophobic carbon pretreated by PTFE led to an increase in proton transport resistance, due to the extended transport path of the reactants. Further, a structure with the gradient distribution of PTFE was designed. It is shown that when PTFE was located near the GDL, the oxygen transport resistance could be further decreased within the CCL and a fast gas-liquid transport channel was constructed. We believe that this work can provide new ideas for the optimization and design of the CL structure.

Acknowledgments

This work was supported by theNational Natural Science Foundation of China (Grant Nos. 21832004 and 21773175).

References

[1] Alaswad A, Baroutaji A, Achour H, Carton J, Al Makky A, Olabi A G. Developments in fuel cell technologies in the transport sector[J]. Int. J. Hydrog. Energy, 2016, 41(37): 16499−16508.

[2] Chen W H, Chen S L. Effect of ink solvents on low-Pt loading proton exchange membrane fuel cell performance [J]. Acta Phys.-Chim. Sin., 2019, 35(5): 517−522.

[3] Liu Q S, Lan F C, Chen J Q, Zeng C J, Wang J F. A review of proton exchange membrane fuel cell water management: membrane electrode assembly[J]. J. Power Sources, 2022, 517: 230723.

[4] Wu C W, Zhang W, Han X, Zhang Y X, Ma G J. A systematic review for structure optimization and clamping load design of large proton exchange membrane fuel cell stack[J]. J. Power Sources, 2020, 476: 228724.

[5] Wang Y, Diaz D FR, Chen K S, Wang Z, Adroher X C. Materials, technological status, and fundamentals of PEM fuel cells - a review[J]. Mater. Today, 2020, 32: 178−203.

[6] Wang X R, Ma Y, Gao J, Li T, Jiang G Z, Sun Z Y. Review on water management methods for proton exchange membrane fuel cells[J]. Int. J. Hydrog. Energy, 2021, 46(22): 12206−12229.

[7] Avcioglu G S, Ficicilar B, Bayrakceken A, Eroglu I. High performance PEM fuel cell catalyst layers with hydrophobic channels[J]. Int. J. Hydrog. Energy, 2015, 40(24): 7720−7731.

[8] Chi B, Hou S Y, Liu G Z, Deng Y J, Zeng J H, Song H Y, Liao S J, Ren J W. Tuning hydrophobic-hydrophilic balance of cathode catalyst layer to improve cell performance of proton exchange membrane fuel cell (PEMFC) by mixing polytetrafluoroethylene (PTFE)[J]. Electrochim. Acta, 2018, 277: 110−115.

[9] Chi B, Ye Y K, Lu X Y, Jiang S J, Du L, Zeng J H, Ren J W, Liao S J. Enhancing membrane electrode assembly performance by improving the porous structure and hydrophobicity of the cathode catalyst layer[J]. J. Power Sources, 2019, 443: 227284.

[10] Wang M, Chen M, Yang Z Y, Liu G C, Lee J K, Yang W, Wang X D. High-performance and durable cathode catalyst layer with hydrophobic C@PTFE particles for low-Pt loading membrane assembly electrode of PEMFC[J]. Energy Conv. Manag., 2019, 191: 132−140.

[11] Cai X, Lin R, Wang H, Liu S C, Zhong D. One simple method to improve the mass transfer of membrane electrode assembly to realize operation under wide humidity [J]. J. Power Sources, 2021, 506: 230185.

[12] Roh C W, Choi J, Lee H. Hydrophilic-hydrophobic dual catalyst layers for proton exchange membrane fuel cells under low humidity[J]. Electrochem. Commun., 2018, 97: 105−109.

[13] Qiu Y L, Zhang H M, Zhong H X, Zhang F X. A novel cathode structure with double catalyst layers and low Pt loading for proton exchange membrane fuel cells[J]. Int. J. Hydrog. Energy, 2013, 38(14): 5836−5844.

[14] Deng R Y, Xia Z X, Sun R L, Wang S L, Sun G Q. Nanostructured ultrathin catalyst layer with ordered platinum nanotube arrays for polymer electrolyte membrane fuel cells[J]. J. Energy Chem., 2020, 43: 33−39.

[15] Yakovlev Y V, Lobko Y V, Vorokhta M, Nováková J, Mazur M, Matolínová I, Matolín V. Ionomer content effect on charge and gas transport in the cathode catalyst layer of proton-exchange membrane fuel cells[J]. J. Power Sources, 2021, 490: 229531.

[16] Xue Q, Li J K, Yang Z Y. Synergistically improving the activity, antipoisonous ability, and long-term stability of Pt to methanol oxidation through developing favorable graphene-based supports[J]. Langmuir, 2017, 33(4): 872−880.

质子交换膜燃料电池阴极催化层疏水性优化

陈浩杰，唐美华，陈胜利*
武汉大学化学系，武汉 430072

摘要

本文采用 CCM 法（catalyst coated membrane）技术，结合单电池极化曲线、电化学阻抗谱、极限电流法和表面接触角等多种表征技术，系统研究了直接聚四氟乙烯（PTFE）分子添加以及 PTFE 修饰的疏水性碳（PTFE@XC72）等不同疏水化方法对质子交换膜燃料电池（PEMFC）的阴极催化层电化学性能、氧气传输阻抗和质子传输阻抗的影响。在此基础上，通过构建 PTFE 梯度化疏水性结构来进一步优化 PEMFC 的性能。结果表明，与添加 PTFE@XC72 相比，直接添加适量的 PTFE 分子对膜电极（MEA）性能提升效果更为显著，这主要与该疏水结构可在维持高速质子传导的同时，极大降低催化层的氧气传输阻抗有关。当直接添加的 PTFE 与催化层中碳载体的质量比为 0.1 时，MEA 呈现最好的性能。在添加 PTFE@XC72 的 MEA 中，由于额外的碳颗粒导致催化层厚度增加，延长了反应物质的传输路径，从而使得质子传输阻抗和氧气传输阻抗均上升。在此基础上，通过在催化层不同位置直接添加 PTFE 构建梯度化疏水性结构。结果表明，当适量 PTFE 靠近催化层与气体扩散层界面分布时，MEA 呈现最好的性能，峰值功率密度比未经疏水性处理的膜电极高接近 20%，氧气传输阻抗大幅降低。

关键词：质子交换膜燃料电池；阴极催化层；聚四氟乙烯；疏水性；氧气传输阻抗